JPEDAV (2009) 30:254–257
DOI: 10.1007/s11669-009-9505-2
1547-7037 ©ASM International

Study on the Solidus Line in Sn-Rich Region of Sn-In Phase Diagram

C.-H. Yeh, L.-S. Chang, and B. Straumal

(Submitted November 21, 2008)

Binary phase diagrams are important tools for designing desired alloys. In the Sn-rich region of the Sn-In alloy phase diagram, the solidus line appears as a dotted line in current literature plots to indicate uncertainty. The contour of the solidus has now been clarified as a result of the present investigation. Four alloys, $Sn_{70}In_{30}$, $Sn_{75}In_{25}$, $Sn_{80}In_{20}$, and $Sn_{85}In_{15}$ were melted at 300 °C for 10 h and annealed between 120 and 200 °C in the (L + γ) two-phase region. The morphology and chemical compositions of annealed specimens were analyzed using both field emission scanning electron spectroscopy and energy-dispersive x-ray spectrometry. The results reveal that the liquid phase, initially appearing at the eutectic temperature, invades the solid along grain boundaries with penetration gradually increasing with increasing annealing temperature and a granular structure form. The average compositions in grains of $Sn_{70}In_{30}$, $Sn_{75}In_{25}$, $Sn_{80}In_{20}$, and $Sn_{85}In_{15}$ specimens correspond to the solidus concentrations, and the solidus line and (β + γ)/γ phase boundary can be determined as a fit to these temperature-composition points.

Keywords binary system, grain boundary wetting, phase diagram, Sn-In alloy, solidus line

1. Introduction

Since 2006, the European Union (EU) has required that imported electric devices must be Pb-free due to environmental considerations and health concerns. Gradually, the most commonly used solder, Pb-Sn alloy, has been replaced by other Sn-based component materials, such as Bi-Sn, Ag-Sn, Sn-In, Sn-In-Bi, and Sn-In-Zn, and so forth.[1-4] In order to develop new solder alloys, materials engineers need alloy phase diagram information, such as melting points, liquidus and solidus data phase transition temperatures, phase compositions, and phase structures at defined temperatures and compositions. Furthermore, alloy phase diagrams can also be used to forecast performance and properties of alloy materials under specified conditions of application.

Tin-indium alloys are low-temperature alloys and are commonly applied to replace Pb-Sn solders. Examples of other applications include uses for cryogenic environments, for step soldering, and in heat-sensitive devices.[5] In 1964, Heumann and Alpaut[6] proposed the currently accepted Sn-In phase diagram. Other investigators[7-11] studied phase structures and phase composition ranges.

C.-H. Yeh and **L.-S. Chang**, Department of Materials Science and Engineering, National Chung Hsing University, 40227 Taichung, Taiwan, ROC; **B. Straumal**, Institute of Solid State Physics, Russian Academy of Sciences, Chernogolovka, Moscow District 142432, Russia. Contact e-mails: d9366101@mail.nchu.edu.tw, lschang@dragon.nchu.edu.tw, and straumal@issp.ac.ru.

To refine the phase equilibria between liquid and solid phases, Predel and Gödecke[8] used differential thermal analysis (DTA) to investigate the liquidus and solidus temperatures in the Sn-rich region. Later, Evans and Prince also used DTA, but added tensile testing to determine the liquidus and solidus boundaries over the entire composition range.[9] Although their results provided some information in the Sn-rich region, the (L + γ)/γ solidus line remained ill defined and plotted as a dashed line in the extensive compilation of 1990.[12]

There also exists uncertainty with regard to the (β + γ)/γ solvus, with significant differences occurring among results from several investigations. Heumann and Alpaut[6] reported that the high-temperature techniques of the (β + γ)/γ phase boundary was about 77 at.% Sn. The same boundary reported by Wojtaszek and Kuzyk[10] was 75 at.% Sn at 80 °C and 76.5 at.% Sn at 110 °C. Lee et al.[10] reported the high-temperature end of the boundary to be at 76.8 at.% Sn.[10] On the other hand, Cakir and Alpaut[11] suggested that the (β + γ)/γ phase boundary should contact the eutectic limits near 72 at.% Sn; this value was determined from electromotive force (emf) measurements with alloys. This difference of ~5 at.% Sn in the (β + γ)/γ upper phase boundary is significant. Thus, a second purpose of this study was to verify the locus of the junction of the (L + γ)/γ solidus, the (β + γ)/γ solvus, and the Sn-rich end of the eutectic.

2. Experimental

Four proportions of Sn (99.999%) and In (99.999%) were sealed under argon atmosphere into quartz tubes. The Sn-30, Sn-25, Sn-20, and Sn-15 (at.%) In alloys, noted as $Sn_{70}In_{30}$, $Sn_{75}In_{25}$, $Sn_{80}In_{20}$, and $Sn_{85}In_{15}$ were prepared by melting and holding at 300 °C for 10 h and homogenized at

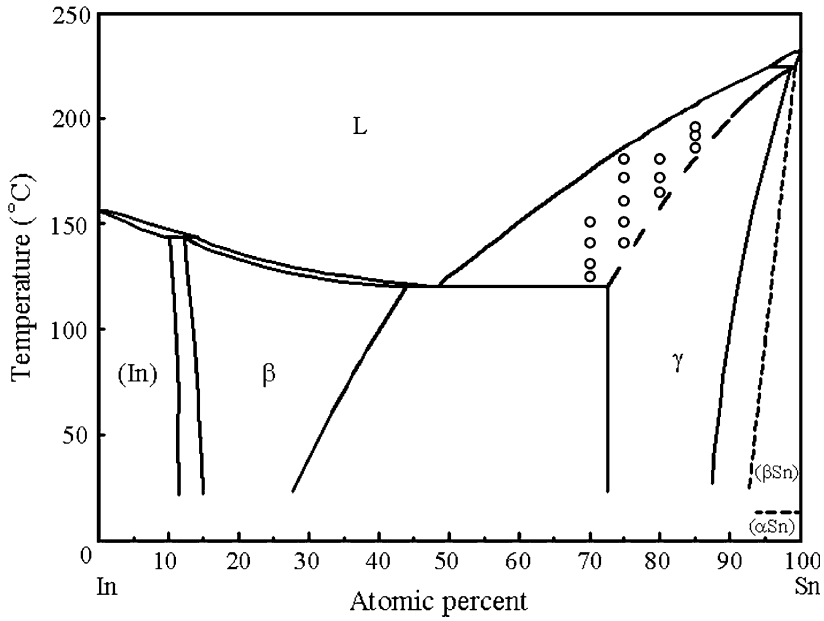

Fig. 1 The Sn-In phase diagram[12] with annealing points ($Sn_{70}In_{30}$: 125, 131, 141, and 151 °C; $Sn_{75}In_{25}$: 141, 151, 161, 172, and 181 °C; $Sn_{80}In_{20}$: 165, 172, and 181 °C; $Sn_{85}In_{15}$: 186, 192, and 196 °C)

100 °C for 24 h. Each alloy of a given composition was then sliced into several specimens. In order to obtain uniform microstructures, the specimens were plasticly deformed by light blows with a hammer and annealed at 110-120 °C for 20 h.

These Sn-rich alloys were annealed above 120 °C eutectic temperature in a furnace for 24 h to approach the phase equilibrium (Fig. 1) and quenched in salt-saturated ice water (−10 °C) and liquid nitrogen. The deviation of annealing temperatures was controlled at ±1 °C. After annealing, clear surfaces of specimens were prepared by an electropolishing instrument (Model Tenupol-5, Struers Corporation, Ballerup, Denmark). The polishing solution contained 70% $HClO_4$ and ethyl alcohol, and the polishing voltage was 30 V.

The microstructures of specimens were observed with a field emission scanning electron microscopy (FESEM, JSM-6700F, JEOL Instrument, Tokyo, Japan). The chemical compositions of about 20 grains in each specimen were analyzed by an energy-dispersive x-ray spectrometer (EDXS, INCA Energy 400, Oxford Instrument, Oxfordshire, UK) for each specimen. The acceleration voltage of EDXS analysis was 15 kV. The sampling time was 60 s. The composition data for each specimen were averaged and placed in the Sn-In phase diagram.

3. Results and Discussion

Figure 2(a) shows the microstructure of $Sn_{70}In_{30}$ specimen, after annealing for 24 h at 125 °C, just 5 °C above the eutectic temperature. All solid grains are γ phase, and the granular structure can be clearly observed. When the annealing temperature increases to the (liquid + γ) two-phase region, the liquid phase first appears at the triple junction and then penetrates into partial grain boundaries and continues until the solid grains could be separated from each other by the liquid phase at boundaries. This phenomenon is called the "grain-boundary wetting transition" and is an important interfacial phenomenon.[13] The wetting transition at triple junctions and grain boundaries follows the thermodynamic criteria, in which, respectively, the triple junction energy should be higher than solid-liquid interfacial energy[14]

$$\sigma_{TJ} > \sqrt{3}\sigma_{SL} \quad \text{(Eq 1)}$$

and the GB energy, σ_{GB} should be higher than twice the value of solid-liquid interfacial energy[15]

$$\sigma_{GB} > 2\sigma_{SL} \quad \text{(Eq 2)}$$

According to the lever rule, the quantity of liquid phase increases as the annealing temperature increases in the (liquid + γ) region. As a result, more and more grain boundaries were wetted by the liquid phase and the thickness of liquid layers increased gradually (Fig. 2b, c). After rapid quenching, the liquid layers solidified as a dendritic mixture of β and γ phases. When the annealing temperature approached the liquidus line, the liquid phase invaded the grains and occupied the predominant area of specimen (Fig. 2e). The aforementioned transitive behavior also occurred in $Sn_{75}In_{25}$, $Sn_{80}In_{20}$, and $Sn_{85}In_{15}$ alloys.

The solidus line (dotted line in Fig. 1) in the Sn-rich side of the Sn-In phase diagram remained indefinite until now. It was determined by measuring the chemical composition of solid-phase grains in samples annealed at different temperatures in the (liquid + γ) two-phase region. The composition of liquid and solid phase corresponded to the liquidus and

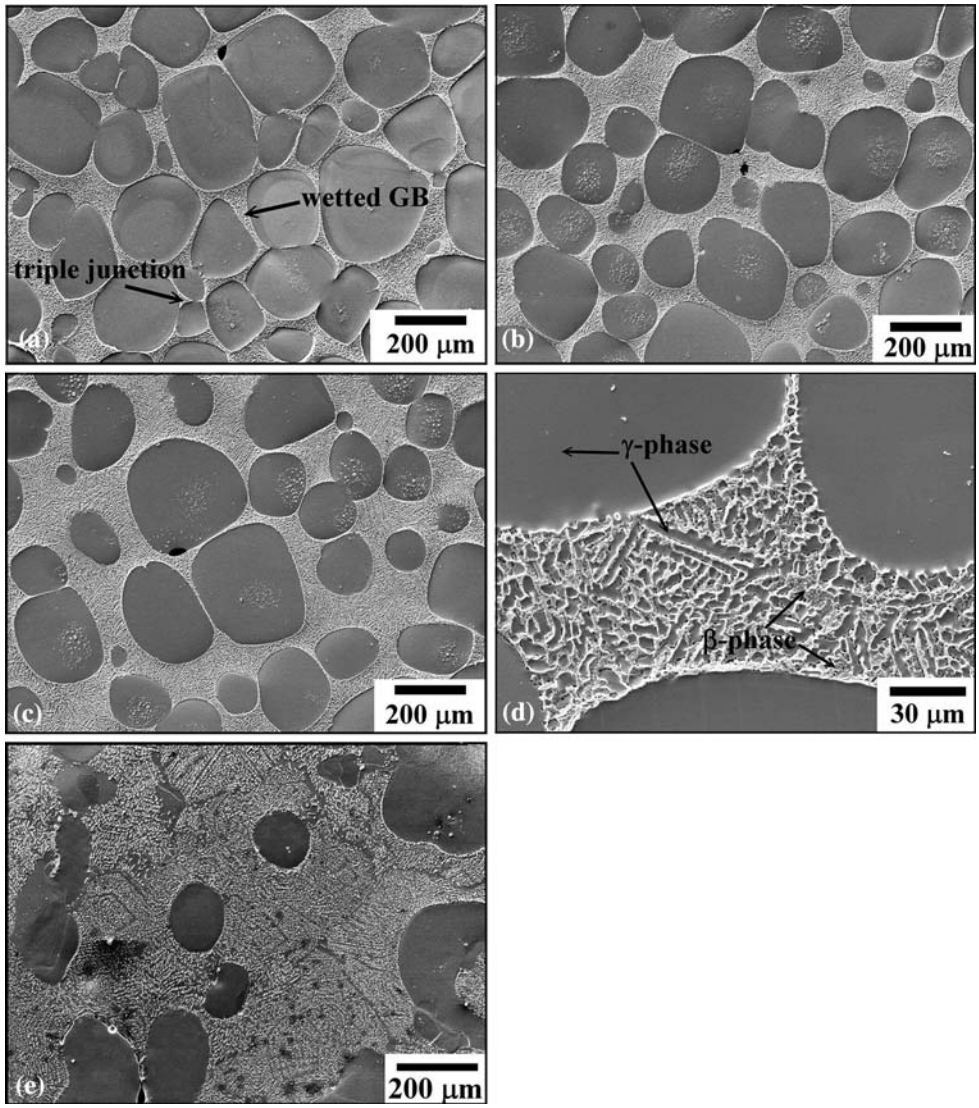

Fig. 2 Micrographs of the $Sn_{70}In_{30}$ specimens after annealing at (a) 125 °C, (b) 141 °C, (c, d) 151 °C and $Sn_{75}In_{25}$ specimens after annealing at (e) 181 °C for 24 h

solidus lines, respectively, at a certain temperature in the (liquid + γ) two-phase region. Table 1 contains the average compositions of grains in the Sn-rich alloys after annealing and quenching. The results are indicated in the Sn-In phase diagram (Fig. 3). The areas for the analysis were chosen inside solid grains, and the results reveal that the average compositions of grains in $Sn_{70}In_{30}$, $Sn_{75}In_{25}$, $Sn_{80}In_{20}$, and $Sn_{85}In_{15}$ specimens increased with increasing annealing temperature and were close to the solidus line proposed previously between 160 and 200 °C. Below 160 °C, the compositions of grains deviated from the solidus line and shifted to higher Sn contents. The solid phase composition of $Sn_{70}In_{30}$ specimen is 76.66 at.% at 125 °C. These experimental data indicate that the (β + γ)/γ phase boundary ought to be approximately 76.5 at.% Sn, which was similar with the experimental results from Evans and Lee. It is shown that the position of solidus line can be verified and the dotted line can be replaced by a solid line in Sn-rich region of Sn-In phase diagram.

4. Conclusions

The chemical composition of solid phase in the $Sn_{70}In_{30}$, $Sn_{75}In_{25}$, $Sn_{80}In_{20}$, and $Sn_{85}In_{15}$ alloys annealed at different temperatures were investigated in the (liquid + γ) region. The granular structure was observed by FE-SEM, and the liquid phase appeared at the triple junction and grain boundaries. When the annealing temperature increases, the quantity of liquid phase increases and the liquid invades the solid grains. According to the compositions of grains measured by EDXS analysis, the solidus line and the (β + γ)/γ phase boundary can be verified in the Sn-rich

Table 1 The average compositions of solid phase grains in $Sn_{70}In_{30}$, $Sn_{75}In_{25}$, $Sn_{80}In_{20}$, and $Sn_{85}In_{15}$ alloys after annealing treatment

Alloys	Annealing temperature, °C	Composition of solid-phase grains, at.%	
		Sn	In
$Sn_{70}In_{30}$	125	76.66	23.34
	131	77.83	22.17
	141	78.42	21.58
	151	80.04	19.96
$Sn_{75}In_{25}$	141	77.91	22.09
	151	79.30	20.70
	161	81.24	18.76
	172	82.86	17.14
	181	85.73	14.27
$Sn_{80}In_{20}$	165	81.06	18.94
	172	81.44	18.56
	181	84.85	15.15
$Sn_{85}In_{15}$	186	86.08	13.92
	192	87.82	12.18
	196	88.13	11.87

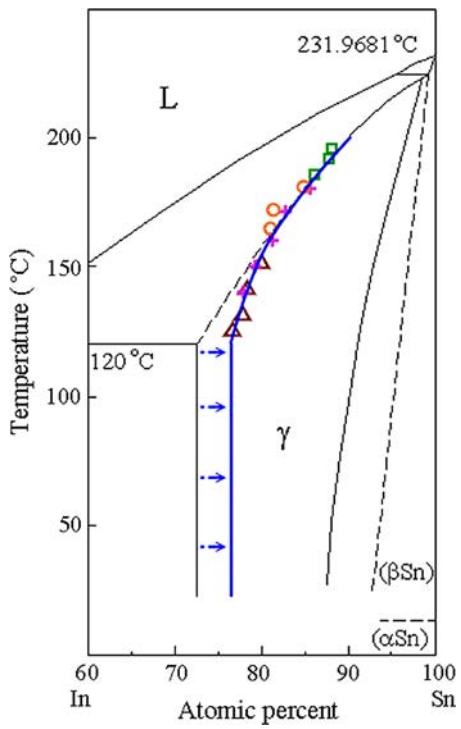

Fig. 3 The (liquid + γ) two-phase region of Sn-In phase diagram (Δ, $Sn_{70}In_{30}$; +, $Sn_{75}In_{25}$; ○, $Sn_{80}In_{20}$; □, $Sn_{85}In_{15}$)

region of the Sn-In phase diagram. The (β + γ)/γ phase boundary ought to be 76.5 at.% Sn.

Acknowledgments

This work was financially supported by the Russian Foundation for Basic Research under the contract 05-03-90578 and National Scientific Council of Taiwan under the contracts NSC 96-2218-E-005-015.

References

1. H. Ipser, H. Flandorfer, Ch. Luef, C. Schmetterer, and U. Saeed, Thermodynamics and Phase Diagrams of Lead-Free Solder Materials, *J. Mater. Sci.: Mater. Electron.*, 2007, **18**, p 3-17
2. T. Laurila, V. Vuorinen, and J.K. Kivilahti, Interfacial Reactions Between Lead-Free Solders and Common Base Materials, *Mater. Sci. Eng.*, 2005, **R 49**, p 1-60
3. N. Moelans, K.C. Hari Kumar, and P. Wollants, Thermodynamic Optimization of the Lead-Free Solder System Bi-In-Sn-Zn, *J. Alloys Compd.*, 2003, **360**, p 98-106
4. L.C. Prasad, Y. Xie, and A. Mikula, Lead Free Solder Materials In-Sn-Zn System, *J. Non-Cryst. Solids*, 1999, **250-252**, p 316-320
5. D.-G. Kim and S.-B. Jung, Interfacial Reactions and Growth Kinetics for Intermetallic Compound Layer Between In-48Sn Solder and Bare Cu Substrate, *J. Alloys Compd.*, 2005, **386**, p 151-156
6. T. Heumann and O. Alpaut, Das Zustandsdiagramm Indium-Zinn, *J. Less-Common Met.*, 1964, **6**, p 108-117, in German
7. O. Nittono, H. Iwasaki, and Y. Koyama, Phase Changes and Shape Memory Effect in In-Sn Alloy Crystals, *Nippon Kinzoku Gakkaishi*, 1980, **44**, p 899-907, in Japanese
8. B. Predel and T. Gödecke, Das Dreistoffsystem Zinn-Indium-Thallium, *Z. Metallkd.*, 1975, **66**, p 654-659, in German
9. D.S. Evans and A. Prince, Alloy Phase Diagrams, *MRS Symposium Proceedings*, L.H. Bennett, T.B. Massalski, and B.C. Giessen, Eds., Elsevier North-Holland, Amsterdam, **19**, 1983, p 389
10. B.-J. Lee, C.-S. Oh, and J.-H. Shim, Thermodynamic Assessments of the Sn-In and Sn-Bi Binary Systems, *J. Electron. Mater.*, 1996, **25**, p 983-991
11. O. Cakir and O. Alpaut, Thermodynamic Properties of Solid In-Sn Alloys, *J. Less-Common Met.*, 1988, **141**, p 11-27
12. T.B. Massalski, H. Okamoto, P.R. Subramanian, and L. Kacprzak, Eds., *Binary Alloy Phase Diagram*, ASM International, Materials Park, OH, 1990, p 2295-2296
13. B. Straumal and B. Baretzky, Grain Boundary Phase Transitions and Their Influence on Properties of Polycrystals, *Interface Sci.*, 2004, **12**, p 147-155
14. B.B. Straumal, O. Kogtenkova, and P. Zięba, Wetting Transition of Grain-Boundary Triple Junctions, *Acta Mater.*, 2008, **28**, p 925-933
15. C.S. Smith, Grains, Phases, and Interfaces: An Interpretation of Microstructure, *Trans. Metall. Soc. AIME*, 1948, **175**, p 15-51